Journal of Magnetic Resonance 246 (2014) 130–135

Contents lists available at ScienceDirect

Journal of Magnetic Resonance

journal homepage: www.elsevier.com/locate/jmr

Evidence for the light hole in GaAs/AlGaAs quantum wells from optically-pumped NMR and Hanle curve measurements

Erika L. Sesti [a], Wieland A. Worthoff [b], Dustin D. Wheeler [a], Dieter Suter [b], Sophia E. Hayes [a,*]

[a] Department of Chemistry, Washington University in St. Louis, St. Louis, MO 63130, United States
[b] Fakultät Physik, Technische Universität Dortmund, 44221 Dortmund, Germany

ARTICLE INFO

Article history:
Received 29 April 2014
Revised 2 July 2014
Available online 30 July 2014

Keywords:
Optically-pumped NMR
OPNMR
^{69}Ga NMR
Hanle curve
GaAs/AlGaAs quantum well
Light hole

ABSTRACT

Optically-pumped ^{69}Ga NMR (OPNMR) and optically-detected measurements of polarized photoluminescence (Hanle curves) show a characteristic feature at the light hole-to-conduction band transition in a GaAs/$Al_xGa_{1-x}As$ multiple quantum well sample. OPNMR data are often depicted as a "profile" of the OPNMR integrated signal intensity plotted versus optical pumping photon energy. What is notable is the inversion of the sign of the measured ^{69}Ga OPNMR signals when optically pumping this light hole-to-conduction band energy in OPNMR profiles at multiple external magnetic fields (B_0 = 4.7 T and 3 T) for both σ^+ and σ^- irradiation. Measurements of Hanle curves at B_0 = 0.5 T of the same sample exhibit similar phase inversion behavior of the Hanle curves at the photon energy for light hole excitation. The zero-field value of the light-hole state in the quantum well can be predicted for the quantum well structure using the positions of each of these signal-inversion features, and the spin splitting term in the equation for the transition energy yields consistent values at 3 magnetic fields for the excitonic *g*-factor (g^{ex}). This study demonstrates the application of OPNMR and optical measurements of the photoluminescence to detect the light hole transition in semiconductors.

1. Introduction

Optically-pumped NMR (OPNMR) has been demonstrated on multiple semiconductor systems including GaAs [1–7], InP [8–13], CdS [14], and Si [15,16]. OPNMR utilizes the hyperfine coupling between optically-oriented electrons and the surrounding nuclear spins, and a number of reviews discuss the underlying physics governing these processes [3,17,18]. OPNMR results in high spin polarization of the small irradiation volumes that are afforded in semiconductor thin films and in materials, where the penetration depth of the light can limit the number of nuclear spins that can be accessed via optical irradiation [17,19,20].

Hanle curves depict the decay of polarized photoluminescence from semiconductor quantum wells as some perturbation is applied, such as sweeping an external magnetic field [21]. The technique is commonly used to measure the radiative lifetime and spin relaxation of electrons in semiconductors [22]. Hanle curves also find applications in astronomy [23] and semiconductor physics [24]. A review concerning this method in semiconductors can be found in reference [25].

Several groups of researchers have used the photon-energy dependence of the OPNMR signals as a probe of various phenomena in bulk GaAs, such as helicity asymmetry [19,26], photoconduction [20,27], hyperfine shift [19], and for our group specifically to probe spin splitting in the valence band [4]. In contrast, the photon energy-dependence of GaAs/$Al_xGa_{1-x}As$ quantum well OPNMR spectra has been less extensively reported, with only a single publication showing the coincidence of photoluminescence excitation and OPNMR signal intensities [28].

We have examined the OPNMR signals from ^{69}Ga spins in GaAs/$Al_xGa_{1-x}As$ quantum wells (hereafter "QWs") to probe the photophysical processes governing polarization of the nuclei at specific optical photon energies. We are able to conduct experiments at multiple external magnetic fields (B_0) in order to examine the photon-energy dependence of features observed by OPNMR. Hanle curve measurements offer the opportunity for a third low-magnetic field measurement at 0.5 T. The ability to conduct experiments at multiple external magnetic fields allows the identification of the light-hole transition that arises from the splitting of the valence-band light-hole energy levels, and ultimately extraction of a zero-field value for the energy of the light-hole valence band state for these particular quantum wells. In general, transitions originating from the light-hole subband are not easy to resolve. The presence of the light hole-to-conduction band

* Corresponding author.
E-mail address: hayes@wustl.edu (S.E. Hayes).

http://dx.doi.org/10.1016/j.jmr.2014.07.001
1090-7807/

transition is observed in photoluminescence excitation [29], through optical cyclotron resonance [30], and magneto-optical Kerr rotation [31] but the light-hole transition is often difficult to deconvolute due to band mixing (i.e., between light-hole and heavy-hole states).

2. Experimental

2.1. Sample

A multiple quantum well sample was grown by MBE, consisting of 60 GaAs quantum wells each with a thickness of 16.9 nm separated by 24.5 nm $Al_{0.31}Ga_{0.69}As$ barriers. The base is a single-crystal GaAs substrate, and the growth of this sample was accompanied by superlattice structures (that are not resonant with the laser wavelengths used here) both above and below the 60 quantum wells. The superlattices are (twenty 4.4 nm GaAs layers separated by 4.9 nm $Al_{0.31}Ga_{0.69}As$ layers). The bandgap energies of these MBE-grown structures at a temperature of 6 K are 1.5325 eV for 16.9 nm GaAs/AlGaAs quantum wells, and approximately 1.60 eV for the superlattice structure. The superlattice was grown on the substrate to create an ideal growth surface for the quantum wells. A second superlattice above the quantum wells helps to trap lattice defects [32] and was grown to obtain a symmetric structure. (The full structure from top to bottom is GaAs base – superlattice – 60 quantum wells – superlattice – 10 nm sacrificial GaAs layer (for oxidation)). This sample was grown by Dr. Soheyla Eshlaghi in the group of Prof. Andreas Wieckat the Ruhr Universtät in Bochum, Germany.

2.2. OPNMR

Experiments were conducted on a single-channel tank circuit NMR probe, designed to operate at cryogenic temperatures. The sample was mounted on a sapphire rod to act as a heat sink using Apiezon Type N grease, inside a helium recirculating cryostat (Janis-SHI 950) where the sample is in contact with static exchange gas, to maintain a sample temperature of 6 K ± 0.3 K. Experiments were conducted in one of two horizontal-bore magnets at 3 T or 4.7 T.

^{69}Ga OPNMR experiments were carried out at a Larmor frequency of 48.04 MHz (for B_0 = 4.7 T) and 30.773 MHz (for B_0 = 3.0 T). The spectra were collected using a pulse sequence consisting of a saturating radio-frequency (rf) train (SAT), followed by a period of continuous wave laser irradiation (τ_L = 60 s), a single $\pi/2$ rf pulse, and signal acquisition (ACQ): SAT – τ_L – $\pi/2$ – ACQ. Four transients using phase cycling were recorded for each OPNMR spectrum. The SAT sequence consists of a train of pulses with 3 ms delays between them, designed to saturate any magnetization that builds up between experiments. Therefore, any signal that develops is primarily due to optical pumping under light irradiation (τ_L) after that SAT sequence. Typical $\pi/2$ pulse lengths were 5 μs. The laser light used for optical pumping was only shuttered during the saturation train and acquisition.

The optical excitation source was a tunable continuous wave Ti:Sapphire frequency-stabilized ring laser (Coherent 899-21, estimated ~30 MHz linewidth) pumped by a 532 nm solid-state diode laser (Specta Physics Millenia X). The laser output was passed through a quarter wave retarder centered at 790 nm. A spectrometer with 0.01 nm resolution (Bristol 521 Wavelength Meter) was used to measure wavelength. Laser power was varied from 100 mW to 200 mW with a spot size of 2 ± 0.5 mm. The sample was irradiated parallel to B_0, along a direction normal to the QW surface, coincident with the direction of MBE growth such that the plane of the QWs are perpendicular to B_0.

2.3. Hanle curves

Measurements of Hanle curves, the decay of polarized photoluminescence emitted from the sample under the influence of sweeping an external magnetic field, were performed after optical pumping at an external magnetic field of 0.5 T. Nuclear fields were prepared at a magnetic field of 0.5 T for 300 s, at desired photon energies (805.4–808.5 nm) with σ^+ or σ^- light. The external field was produced with a Bruker electromagnet (sweep range of 0–1.5 T) and was also used to sweep the field from 0–1 T to acquire a Hanle curve. Therefore, the overall Hanle experiments consist of preparing the nuclear field at 0.5 T, then the external magnetic field is set to 0 T and swept from 0–1 T. A tunable continuous wave Ti:Sapphire laser (Coherent 899-01, ~5 GHz linewidth), which was pumped with a 532 nm Verdi V8 solid-state laser, was used as an optical excitation source followed by a quarter wave retarder to achieve σ^+ and σ^- light. Typical laser excitation powers were 50 mW with an estimated spot size of ~100 μm in the sample. Polarized photoluminescence was collected and recorded by a photoelastic modulator (Hinds Instruments PEM 90), linear polarizer, monochromator (Spex 1794), avalanche photodiode (Hamatsu 5640), lowpass filter (Stanford Research SR640) and lockin amplifier (Stanford Research SR830 DSP) working in conjunction [33]. The sample was kept at a constant temperature of ~4.8 ± 0.2 K in a cold-finger cryostat. Fizeau wavelength meter (New Focus Model 7711) monitored the irradiation wavelength during all the experiments.

3. Results

The measurement of ^{69}Ga OPNMR results in an NMR spectrum arising from the optically-oriented electrons used to polarize the surrounding nuclei. We use two different helicities of light (σ^+ and σ^-) to orient the electrons in conduction-band states with $\sigma^\pm$ photons carrying $\pm\hbar$ angular momentum (IEEE convention), as shown in Fig. 1 below for σ^+ light. As we have shown in publications related to bulk GaAs [2], as the photon energy for optical pumping is incremented, electronic states are accessed which can be mixtures of heavy-hole and light-hole to conduction band transitions. Considering irradiation by σ^+, a lower energy photon will excite the heavy hole transition from the $m_J = -3/2$ state to the $-1/2$ conduction band state. A higher energy photon with the same helicity will excite an electron from the light hole $m_J = -1/2$ state to the $+1/2$ conduction band state, which ultimately means the two optical pumping conditions yield electrons with opposite orientations. The resulting magnetization is thus oriented in the opposite direction and the resulting NMR signal has the opposite sign. These states "encode" the resulting electron spin orientation onto nuclear spins through a Fermi-contact hyperfine interaction [34,35] which is subsequently detected through radio-frequency (NMR) detection of the surrounding nuclei. Here, we report on NMR signals arising from the ^{69}Ga nuclei.

In our experiments, the photon energy for optical pumping of the quantum wells is varied, which leads to fluctuations in both the OPNMR signal intensity and its sign. This plot of OPNMR integrated signal intensity dependence versus photon energy is termed the OPNMR "profile". The OPNMR profile for ^{69}Ga is depicted at different magnetic fields and for both σ^+ and σ^- laser irradiation in Fig. 2.

Here, in the quantum wells, the OPNMR profile exhibits oscillations in the integrated intensity of the signal as a function of photon energy. (Note that the *relative* intensity across a profile is maintained, but it is difficult to compare intensities observed at 4.7 T to those a 3 T, due to differences in probe performance at the different frequencies.) In prior work [2], we described

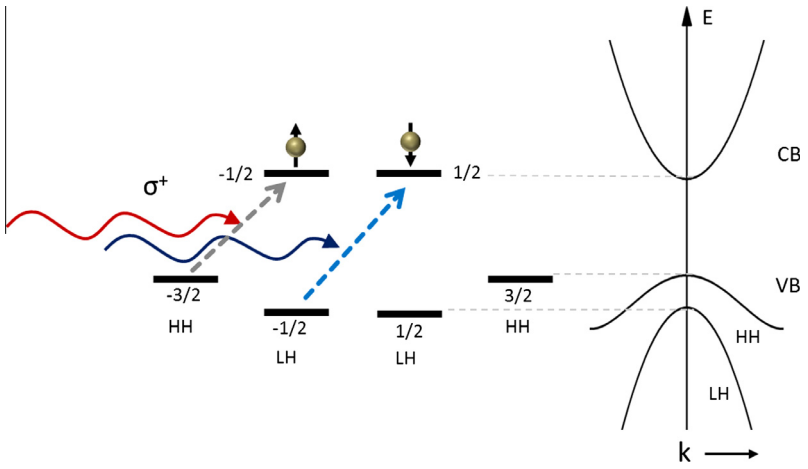

Fig. 1. Schematic band diagram of GaAs quantum wells (and the associated band edge states, approximated by m_j energy levels), showing the allowed transitions at $k = 0$, along with spin orientation of conduction electrons when irradiated with σ^+ light, which carries an angular momentum of +1 unit of ħ. The heavy hole is excited by a lower energy photon, and the light hole is excited by the higher energy one, with the two resulting oriented electrons being in different spin states with respect to each other.

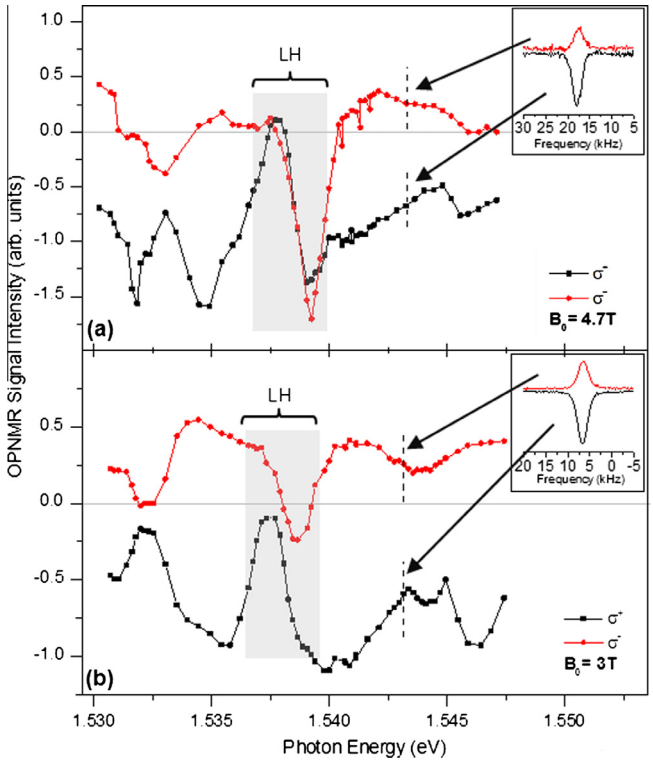

Fig. 2. Experimental ^{69}Ga OPNMR profiles for (a) $B_0 = 4.7$ T and (b) $B_0 = 3.0$ T. Black symbols represent irradiation with σ^+ light, and red symbols represent σ^- light. Each symbol represents the integrated peak intensity for a single OPNMR experiment. The approximate positions of the light-hole (LH) transitions are labeled on each figure as a guide to the eye. The insets show individual OPNMR spectra at 1.54327 eV for each magnetic field (marked by dashed lines). (For interpretation of the references to color in this figure legend, the reader is referred to the web version of this article.)

oscillations in the OPNMR profile of bulk si–GaAs from theoretically predicted electron spin polarization, $P = (n\uparrow - n\downarrow)/(n\uparrow + n\downarrow)$, that reflects populations, n, of the conduction band "spin-up" (↑) and "spin-down" (↓) states. This polarization was determined by calculation of absorption arising from the spin-split band structure in magnetic fields of 4.7 T and 7.05 T.

There is a change in the sign of the OPNMR signals, which is particularly prominent at photon energies where the light-hole states are accessed (near 1.537–1.539 eV). The energies of the maxima are 1.53792 eV for σ^+ and 1.53925 eV for σ^- at 4.7 T, and 1.53770 eV for σ^+ and 1.53867 eV for σ^- at 3 T.

This change of the sign of the signal results in absorptively-phased spectra becoming emissively-phase (or vice-versa). This inversion is large and intense for σ^- irradiation at the energy of the light hole-to-conduction band transition for both magnetic fields, and is less prominent for σ^+ irradiation. While not all of these features in the profile have been assigned (requiring detailed theoretical calculations of the complex GaAs/AlGaAs bandstructure), we are able to identify this particular transition by its optical signature, where the polarized photoluminescence emitted from the quantum well inverts, as expected for the light hole (see Ref. 28 by Miller et al.).

One significant observation is that this large feature (marked by the "LH" label) shifts in energy as a function of magnetic field—the position of the peak where the signal inversion is observed moves to lower energy at 3 T versus 4.7 T.

To confirm these results, low-field (0.5 T) measurements of Hanle curves were measured, in particular across a range of optical-pumping photon energies (Fig. 3). At the position of the light hole, the Hanle curves also invert as this particular state is accessed. The Hanle curve for σ^+ light at lower photon energies inverts to the opposite sign at photon energies near 1.53716 eV (806.59 nm), and for σ^- at 1.53727 eV (806.53 nm). These values each represent the apex of peaks fitted to the data as shown in Fig. 3c. Wavelengths for optical pumping are calibrated ±0.01 nm or 2×10^{-5} eV.

The dependence of this inversion in signals observed by OPNMR and in Hanle curves can be plotted as a function of external magnetic field, B_0. Fig. 4 shows the position of these inversions at the three external magnetic fields (0.5 T, 3.0 T and 4.7 T) for irradiation with σ^+ and σ^- light (black and red symbols, respectively). The solid lines are a linear fit to the data (using Origin), and the lines both converge at a 0 field ($B_0 = 0$ T) at a value of 1.53709 eV. This value agrees well with comparable light hole data for 18 nm at 3.3 T [36], and both 14 nm and 21 nm quantum wells at 0 T [37]. These studies show shifts in the light hole energy in absorption and photoluminescence spectra [38] of GaAs multi-quantum wells.

One can also calculate what the approximate energy-level splitting should be (at $k = 0$, see Fig. 1) between the $m_j = -1/2$ to $+1/2$ (from irradiation with σ^+ light: ε^-) and the $m_j = +1/2$ to $-1/2$ transition (irradiation with σ^- light: ε^+) using Eq. (1) [39]

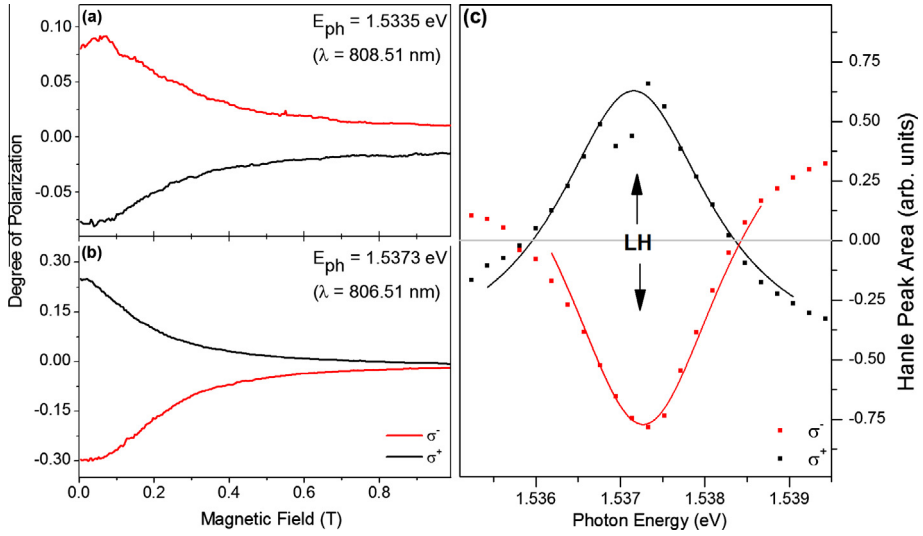

Fig. 3. Hanle curve measurements at the indicated photon energies (a) at 1.5335 eV and (b) at 1.5373 eV. The red plots are for irradiation by σ^- light and the black plots for σ^+ irradiation. The Hanle peaks shown in (b) are inverted relative to those at lower photon energies (as shown in (a)). (c) is a plot of Hanle curve peak areas as a function of photon energy for optical pumping—similar to an OPNMR profile (the solid lines are a guide to the eye). An inversion in the Hanle curves is observed over a range of energies where the light hole-to-conduction band transition is accessed.

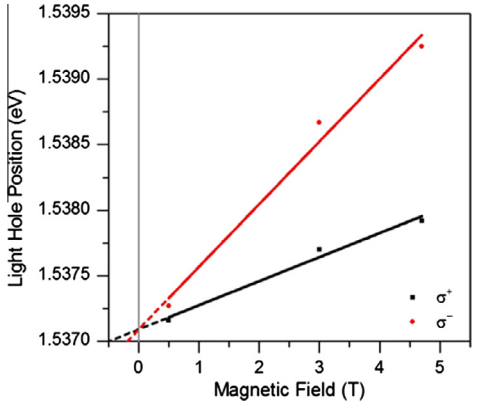

Fig. 4. Plot of the position of the OPNMR and Hanle curve signal inversions at the position of the light-hole to conduction-band transition, as a function of external magnetic field strength, B_0. The red plots are for irradiation by σ^- light and the black plots for σ^+ irradiation. A least squares linear fit to the data shows the two lines converge at the zero-field value of E_{ph} = 1.53709 eV.

$$\varepsilon^{\pm}_{k'k} = \varepsilon_f - \varepsilon_i = \varepsilon_g + \left(n + \frac{1}{2}\right)\hbar(\omega_C + \omega_V) \pm \hbar\gamma B \tag{1}$$

where ε_g is the bandgap at $k = 0$, ω_C and ω_V are the cyclotron frequency of the conduction band and valence band electrons respectively, n is a quantum number that indexes the Landau level of the conduction band state, and $\hbar\gamma B$ is the spin splitting term (where γ is the gyromagnetic ration of the electron). The spin splitting term is defined as $1/2\ \mu_B(g_C + g_V)B$, where μ_B is the Bohr magneton, B is the magnetic field and g_C and g_V are the Landé g-factors for conduction and valence band [40]. Calculated energy splittings between irradiation with σ^+ and σ^- light is expressed by $\Delta\varepsilon$ described by Eq. (2):

$$\Delta\varepsilon = \varepsilon^{+}_{k'k} - \varepsilon^{-}_{k'k} = 2\hbar\gamma B = \mu_B(g_c + g_V)B \tag{2}$$

Splittings from the fit lines in Fig. 4 for the 3 separate magnetic fields, along with the calculated $(g_c + g_v)$ values from Eq. (2) are compared in Table 1.

The familiar conduction electron effective g-factor is −0.44 ($=g_{ebulk} = g_c$) for bulk GaAs and was shown to be equal to approximately −0.3 ($=g_c$) for quantum wells of this width [41].The value for the g-factor here with excitation from the light-hole band consistently returns a value of +5.1. Adapting an expression by Snelling et al., the g-factor for the excitonic transition for light-hole and heavy-hole are different values, which can be written as (respectively) [42]:

Table 1
Data for the energy difference of the light hole-to-conduction band transitions for σ^+ and σ^- irradiation, and the calculated values for the Landé g-factors for each field strength, B_0.

Magnetic field (T)	Experimental energy splittings (meV)	Calculated $g_C + g_V$
0.5	0.15	5.18
3.0	0.88	5.07
4.7	1.39	5.15

$$g^{ex}_{lh} = g_c + g_{lh} \tag{3}$$

$$g^{ex}_{hh} = g_c + g_{hh} \tag{4}$$

Here, g-factors for light hole and heavy hole differ, and these correspond to g_v in Eqs. (1) and (2) above. These expressions suggest a large positive value for g_{lh}, which agrees with the results of the Arora data (an extrapolation) between +6 to +10 [31]. In addition, another light-hole study by Chen et al. also reported a large positive g-factor of +7 for an 18 nm well [43]. These methods are dominantly magneto-optical (i.e. using magneto-optical Kerr effect and reflective difference spectroscopy in a weak magnetic field) to obtain values of the g-factors. As stated in reference [31], for measurements that rely on luminescence, typically only the lowest energy states are occupied by the photo-excited carriers. Consequently, they yield g-factors for confined electron and heavy-hole subbands and not for states at higher energy such as the light-hole subbands. Since measurements of the confined light-hole g-factor is challenging, there still appears to be significant questions regarding correct value.

This linear dependence of the energy of the transition between the light hole and conduction band has a direct analogy to "waterfall plots" from optical magneto-absorption [44]. This linear plot of the energy versus external magnetic field can be ultimately used in

complex computations of band parameters for the sample, but such calculations are dominantly executed for the heavy hole-to-conduction band transition. However, in the case of OPNMR and Hanle measurements of the quantum well, it is the light hole that is most clearly resolved here, due to the change in sign of the signal. Such band parameters that one can obtain (but are beyond the scope of work here) include the conduction-band effective mass (m_c), the light and heavy hole effective masses (m_{lh} and m_{hh}, respectively), the valence-band g factor (g_v), and the conduction-band g factor (g_c), as well as some other parameters used for defining interaction energy and Luttinger parameters [39,44–48]. As seen in literature, values for m_c, m_{lh}, m_{hh}, g_v, and g_c change depending on the specific sample being studied making the flexibility of NMR a useful tool for their analysis [31,49,50]. The methods reported here provide realistic inputs for the light-hole transition that can be used when modeling data for this sample and other GaAs quantum wells that show similar behavior.

4. Conclusions

The light hole-to-conduction band transition in GaAs/AlGaAs quantum wells is marked by an inversion in the sign of the signal for both OPNMR and optical detection of polarized photoluminescence (Hanle curve measurements). This feature moves, as one would expect, as a function of external magnetic fields, and here we report on 4.7 T and 3 T measurements for OPNMR, and 0.5 T for Hanle curves. We extrapolate a zero-field energy of this light hole-to-conduction band transition equal to 1.53709 eV.

The position of the transition energy at these magnetic fields for circularly polarized light (σ^+ and σ^-) can be used by researchers concerned with magnetic-field effects in semiconductors, notably for perturbation of the band structure and as a measure of the g-factors associated with this transition. Here based on the linear plots of the transition energy for each helicity of light, we estimate a g-factor for the excitonic transition from the light hole (g_{lh}^{ex}) of approximately +5.1 to +5.2.

Acknowledgments

This material is based upon work supported by the National Science Foundation under Grant No. (#1206447). W.W. acknowledges support from the German Academic Exchange Service (DAAD).

References

[1] K. Ramaswamy, S. Mui, S. Hayes, Light-induced hyperfine Ga69 shifts in semi-insulating GaAs observed by optically polarized NMR, Phys. Rev. B 74 (2006) 1–4.
[2] K. Ramaswamy, S. Mui, S.A. Crooker, X. Pan, G.D. Sanders, C.J. Stanton, et al., Optically pumped NMR: revealing spin-dependent Landau level transitions in GaAs, Phys. Rev. B 82 (2010) 1–5.
[3] C.R. Bowers, Microscopic interpretation of optically pumped NMR signals in GaAs, Solid State Nucl. Magn. Reson. 11 (1998) 11–20.
[4] A.K. Paravastu, S.E. Hayes, B.E. Schwickert, L.N. Dinh, M. Balooch, J.A. Reimer, Optical polarization of nuclear spins in GaAs, Phys. Rev. B 69 (2004) 1–8.
[5] J.P. King, Y. Li, C.A. Meriles, J.A. Reimer, Optically rewritable patterns of nuclear magnetization in gallium arsenide, Nat. Commun. 3 (2012) 918.
[6] T. Pietrass, A. Bifone, T. Rõõm, E.L. Hahn, Optically enhanced high-field NMR of GaAs, Phys. Rev. B Condens. Matter. 53 (1996) 4428–4433.
[7] J.G. Kempf, M.A. Miller, D.P. Weitekamp, Imaging quantum confinement with optical and POWER (perturbations observed with enhanced resolution) NMR, Proc. Natl. Acad. Sci. USA 105 (2008) 20124–20129.
[8] A. Goto, K. Hashi, T. Shimizu, R. Miyabe, X. Wen, S. Ohki, et al., Optical pumping NMR in the compensated semiconductor InP:Fe, Phys. Rev. B 69 (2004) 1–7.
[9] A. Patel, O. Pasquet, J. Bharatam, E. Hughes, R.C. Bowers, Optical dynamic nuclear polarization in InP single crystal: wavelength and field dependence of NMR enhancement, Phys. Rev. B 60 (1999) R5105–R5108.
[10] K.L. Sauer, C.A. Klug, J.B. Miller, J.P. Yesinowski, Optically pumped InP: nuclear polarization from NMR frequency shifts, Phys. Rev. B 84 (2011) 1–12.
[11] R. Tycko, Optical pumping in indium phosphide: 31P NMR measurements and potential for signal enhancement in biological solid state NMR, Solid State Nucl. Magn. Reson. 11 (1998) 1–9.
[12] R. Tycko, Optical pumping of dipolar order in a coupled nuclear spin system, Mol. Phys. 95 (1998) 1169–1176.
[13] C.A. Michal, R. Tycko, Nuclear spin polarization transfer with a single radio-frequency field in optically pumped indium phosphide, Phys. Rev. Lett. 81 (1998) 3988–3991.
[14] T. Pietraß, M. Tomaselli, Optically pumped NMR in CdS single crystals, Phys. Rev. B 59 (1999) 1986–1989.
[15] A. Verhulst, I. Rau, Y. Yamamoto, K. Itoh, Optical pumping of Si29 nuclear spins in bulk silicon at high magnetic field and liquid helium temperature, Phys. Rev. B 71 (2005) 1–10.
[16] G. Lampel, Nuclear dynamic polarization by optical electronic saturation and optical pumping in semiconductors, Phys. Rev. Lett. 20 (1968) 491–493.
[17] S.E. Hayes, S. Mui, K. Ramaswamy, Optically pumped nuclear magnetic resonance of semiconductors, J. Chem. Phys. 128 (2008) 052203.
[18] R. Tycko, S. Barrett, Optically pumped NMR of semiconductors and two-dimensional electron systems, Encycl. Magn. Reson. 9 (2002) 711–719.
[19] S. Mui, K. Ramaswamy, S.E. Hayes, Physical insights from a penetration depth model of optically pumped NMR, J. Chem. Phys. 128 (2008) 052303.
[20] P. Coles, J. Reimer, Penetration depth model for optical alignment of nuclear spins in GaAs, Phys. Rev. B 76 (2007) 1–11.
[21] L.N. Novikov, G.V. Skrotskii, G.I. Solomakho, The Hanle effect, Sov. Phys. Uspekhi. 17 (1975).
[22] C. Weisbuch, C. Hermann, Optical detection of conduction-electron spin resonance in GaAs, Ga_{1−x}In_{x}As, and Ga_{1−x}Al_{x}As, Phys. Rev. B 15 (1977) 816–822.
[23] R. Ignace, K.H. Nordsieck, J.P. Cassinelli, The Hanle effect as a diagnostic of magnetic fields in stellar envelopes. I. Theoretical results for integrated line profiles, Astrophys. J. 1 (1997) 550–570.
[24] F. Meier, B.P. Zakharchenya, Optical Orientation, North Holland, New York, 1984.
[25] C. Hermann, G. Lampel, V. Safarov, Optical pumping in semiconductors, Ann. Phys. (Paris) 10 (1985) 1117–1138.
[26] P. Coles, Helicity asymmetry of optically pumped NMR spectra in GaAs, Phys. Rev. B 78 (2008) 5–8.
[27] A.K. Paravastu, P.J. Coles, J.A. Reimer, T.D. Ladd, R.S. Maxwell, Photocurrent-modulated optical nuclear polarization in bulk GaAs, Appl. Phys. Lett. 87 (2005) 232109.
[28] S.E. Barrett, R. Tycko, L.N. Pfeiffer, K.W. West, Directly detected nuclear magnetic resonance of optically pumped GaAs quantum wells, Phys. Rev. Lett. 72 (1994) 1368–1371.
[29] R. Miller, A. Gossard, G. Sanders, New evidence of extensive valence-band mixing in GaAs quantum wells through excitation photoluminescence studies, Phys. Rev. B 32 (1985) 8452–8454.
[30] R. Romestain, C. Weisbuch, Optical detection of cyclotron resonance in semiconductors, Phys. Rev. Lett. 45 (1980) 2067–2070.
[31] A. Arora, A. Mandal, S. Chakrabarti, S. Ghosh, Magneto-optical Kerr effect spectroscopy based study of Landé g-factor for holes in GaAs/AlGaAs single quantum wells under low magnetic fields, J. Appl. Phys. 113 (2013) 213505.
[32] H. Jung, A. Fischer, K. Ploog, Photoluminescence of Al{x}Ga{1−x}As/GaAs grown by molecular beam epitaxy, Appl. Phys. A 33 (1984) 97–105.
[33] J.C. Kemp, Polarized Light and its Interaction with Modulating Devices, HINDS International Inc., Hillsboro, 1987.
[34] D. Paget, G. Lampel, B. Sapoval, V.I. Safarov, Low field electron-nuclear spin coupling in gallium arsenide under optical pumping conditions, Phys. Rev. B 15 (1977).
[35] C.D. Jeffries, Dynamic Nuclear Orientation, Interscience, New York, 1963.
[36] P.V. Petrov, Y.L. Ivánov, Experimental observation of giant Zeeman splitting of the light-hole level in a GaAs/AlGaAs quantum well, Semiconductors 47 (2013) 455–456.
[37] R. Dingle, W. Wiegmann, C. Henry, Quantum states of confined carriers in very thin $Al_xGa_{1-x}As$–GaAs–$Al_xGa_{1-x}As$ heterostructures, Phys. Rev. Lett. 33 (1974) 827–830.
[38] C. Weisbuch, R.C. Miller, R. Dingle, A.C. Gossard, W. Wiegmann, Intrinsic radiative recombination from quantum states in GaAs–$Al_xGa_{1-x}As$ Mult-quantum well structures, Solid State Commun. 37 (1981) 219–222.
[39] J.G. Mavroides, Magneto-optical properties, in: F. Abeles (Ed.), Opt. Prop. Solids, American Elsevier Publishing Company Inc., New York, 1972, pp. 351–528.
[40] L.D. Landau, E.M. Lifshitz, Quantum Mechanics, Third, Butterworth-Heinemann, Burlington, MA, 2003.
[41] M. Snelling, G. Flinn, A. Plaut, R. Harley, A. Tropper, R. Eccleston, et al., Magnetic g factor of electrons in GaAs/$Al_xGa_{1-x}As$ quantum wells, Phys. Rev. B Condens. Matter. 44 (1991) 11345–11352.
[42] M. Snelling, E. Blackwood, C. McDonagh, R. Harley, C. Foxon, Exciton, heavy-hole, and electron g factors in type-I GaAs/$Al_xGa_{1-x}As$ quantum wells, Phys. Rev. B Condens. Matter. 45 (1992) 3922–3925.
[43] Y.H. Chen, X.L. Ye, B. Xu, Z.G. Wang, Z. Yang, Large g factors of higher-lying excitons detected with reflectance difference spectroscopy in GaAs-based quantum wells, Appl. Phys. Lett. 89 (2006) 051903.
[44] K. Alavi, R. Aggarwal, S. Groves, Interband magnetoabsorption of In_{0.53}Ga_{0.47}As, Phys. Rev. B 21 (1980) 1311–1315.
[45] C. Pidgeon, R. Brown, Interband magneto-absorption and Faraday rotation in InSb, Phys. Rev. 146 (1966) 575–583.
[46] M. Reine, R. Aggarwal, B. Lax, Stress-modulated magnetoreflectivity of gallium antimonide and gallium arsenide, Phys. Rev. B 5 (1972) 3033–3049.

[47] L.M. Roth, B. Lax, S. Zwerdling, Theory of optical magneto-absorption effects in semiconductors, Phys. Rev. 114 (1959) 90–104.
[48] V.E. Kirpichev, I.V. Kukushkin, V.E. Bisti, K. von Klitzing, K. Eberl, Magnetooptic measurements of the cyclotron mass and g-factor of light holes in GaAs, JETP Lett. 64 (1996) 766–771.
[49] J.C. Maan, G. Belle, A. Fasolino, M. Altarelli, K. Ploog, Magneto-optical determination of exciton binding energy in GaAs-$Ga_{1-x}Al_x$ As quantum wells, Phys. Rev. B 30 (1984) 2253–2256.
[50] R. Miller, D. Kleinman, Excitons in GaAs quantum wells, J. Lumin. 30 (1985) 520–540.